Green Chemistry

PAPER

View Article Online
View Journal | View Issue

Check for updates

Cite this: *Green Chem.*, 2023, **25**, 10447

New conformationally flexible and recyclable aryl iodine catalysts from an inexpensive chiral source for asymmetric oxidations†

Hai-Jie Zhou,[a] Yi-Ping Yao,[a] Tonghui Zhang,[e] Biao Chen,[a] Xu Wang,[a] Hang Zhao,[a] Jie Zeng,[e] Jian-Ai Chen,[a] Xiao Xiao *[a] and Fen-Er Chen *[a,b,c,d,e]

Received 6th July 2023,
Accepted 16th October 2023

DOI: 10.1039/d3gc02429f

rsc.li/greenchem

Published on 24 October 2023. Downloaded on 12/13/2023 3:32:08 AM.

Despite the remarkable advances in the research field of asymmetric catalytic oxidation reactions *via* hypervalent iodines with simple procedures, high level of efficiency and stereoselectivity and the development of their highly scalable, environmentally benign, and sustainable protocols under the greener organocatalysis paradigm for further industrial translations remains a long-standing challenge in synthetic organic chemistry and process engineering over the past few decades. Herein, we design and synthesize a new library of conformationally flexible and recyclable aryl iodine catalysts by utilization of (i) industrial waste (chloramphenicol base) as the scaffold and (ii) inexpensive amino acid residue (threonine) as the chiral source. Our chiral aryl iodine(III) catalysts bearing H-bond donors and a tunable chiral pocket have been successfully applied in diverse, robust asymmetric oxidative transformations, *e.g.*, dearomatization, spirolactonization, direct C(sp^2)–H/C(sp^3)–H cross coupling, and fluoridation. Our processes feature a column isolation-free approach, easy-handling operation, and upscaling synthesis with the catalysts being facilely recycled, in particular *via* precipitation.

Introduction

Hypervalent iodines, possessing peculiar and unique properties, have proven to be versatile, hypotoxic, easily handled, stable, and environmentally benign oxidants in organic synthesis, leading to numerous achievements in "metal-like" oxidative transformations to access significant scaffolds at the same, or even in some cases, a higher level of efficiency than various transition metals.[1–12] In this matter, asymmetric oxidation reactions utilizing chiral organoiodines have presented themselves as a state-of-the-art field, conveying high applicability and versatility in modern organic synthesis.[13–21] The past decade has witnessed tremendous advancements in enantioselective hypervalent iodine catalyses in asymmetric organocatalytic oxidation reactions, which have turned out to be a challenging research area because of the difficulty in achieving higher stereoselectivity at related transition states compared with the metal-catalyzed and enzymatic counterparts.[15–21] Therefore, the development of highly efficient chiral organoiodine catalysts to fulfill various asymmetric transformations and obtain enantiopure structures remains highly sought after.[22–38]

Since the pioneering discovery of chiral iodoarene-catalyzed enantioselective α-oxytosylation reported by Wirth and coworkers in 2007,[39] a variety of C_1- and C_2-symmetric iodoarenes, chiral spiro iodoarenes, and chiral planar iodoarenes have been developed.[17,40–49] Given the emergence of the first C_2-symmetric chiral iodoarene-catalyzed Kita oxidative spirolactonization reported by Ishihara,[40,41] the significant progress for the utilization of these conformationally flexible scaffolds as effective precatalysts to approach diversiform transformations has been well presented due to their suitable chiral environment and *in situ*-generated intramolecular interactions (Fig. 1A).[22–38] The represented structure of the C_2-symmetric chiral iodoarene is derived from substituted lactate, which may react with the oxidant and substrates to form the helical chiral intermediates (*e.g.* **Int-A**) *via* intramolecular n–σ*

[a]*Institute of Pharmaceutical Science and Technology, Collaborative Innovation Center of Yangtze River Delta Region Green Pharmaceuticals, Zhejiang University of Technology, Hangzhou 310014, P. R. China. E-mail: pharmxiao@zjut.edu.cn*
[b]*College of Chemistry and Chemical Engineering, Jiangxi Normal University, Nanchang, 330022, P. R. China*
[c]*Engineering Center of Catalysis and Synthesis for Chiral Molecules, Department of Chemistry, Fudan University, 220 Handan Road, Shanghai 200433, P. R. China. E-mail: rfchen@fudan.edu.cn*
[d]*Shanghai Engineering Center of Industrial Asymmetric Catalysis for Chiral Drugs, Shanghai 200433, P. R. China*
[e]*Pharmaceutical Research Institute, Wuhan Institute of Technology, Wuhan 430205, P. R. China*

†Electronic supplementary information (ESI) available. CCDC 2236217 (**Cat-8**) and 2236218 (**11**). For ESI and crystallographic data in CIF or other electronic format see DOI: **https://doi.org/10.1039/d3gc02429f**

Published on 24 October 2023. Downloaded on 12/13/2023 3:32:08 AM.

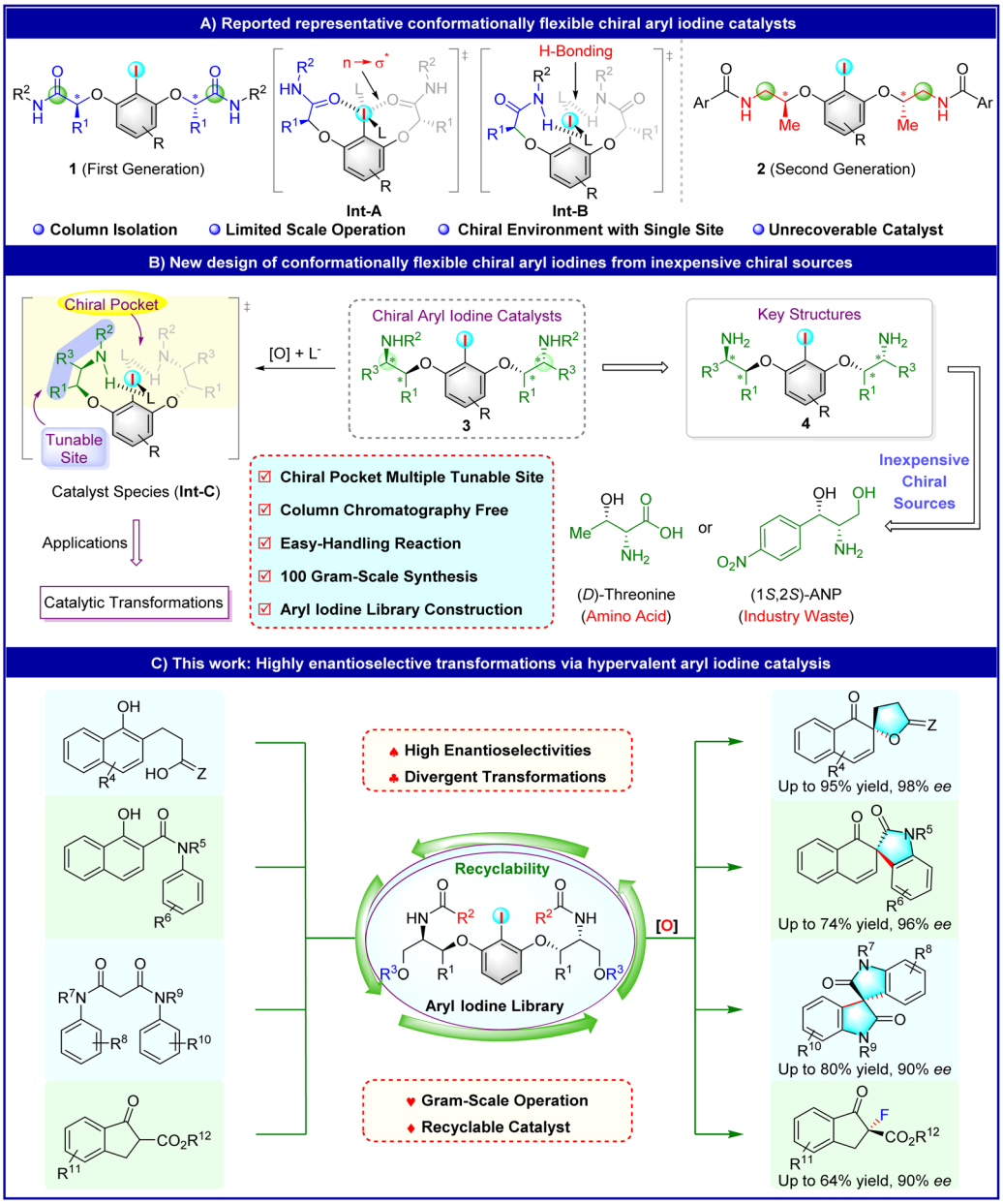

Fig. 1 Schematic of aryl iodine catalyst design and applications.

interactions of the aryl iodine **1** between the Lewis basic group (carbonyl) and the electron-deficient iodine(III) centre or intramolecular H-bond interactions (*e.g.* **Int-B**) of catalyst **1** or **2** between the acidic hydrogen and the iodine(III) ligand.[23,34,50,51] Though these catalyst precursors possess broad applicabilities in numerous exceptional transformations in organic synthesis, some challenges in the catalyst design and preparation remain yet to be solved, limiting the further applications and industrial translations of these catalysts. Synthetically, the large-scale processes to access precatalysts are rare (the reported largest scale process reaches 20 g scale),[52] especially in the second-generation analogue synthesis (within 7 g) due to the fact that column isolation is unavoidable.[51,53–56] Structurally, the limited conventional chiral source made the reported catalysts possess only one chiral centre, which might decrease the richness and tunability of the catalysts' chiral environment, leading to inhibition of their synthetic diversity and reactivities. Practically, all the previous catalysts are unrecoverable without column purification, severely hampering the application of iodine-catalyzed oxidations at the industrial level. Hence, the design and synthesis of a new conformationally flexible catalyst library that features facile availability, high reactivity, and recoverability would be highly acclaimed.

To approach ideal chiral organoiodine catalysts, we intend to install an inexpensive chiral source bearing multi chiral centres on the aryl iodine scaffold (Fig. 1B). Mechanistically,

 This journal is © The Royal Society of Chemistry 2023

Published on 24 October 2023. Downloaded on 12/13/2023 3:32:08 AM.

the precatalyst **3** can be oxidized to form the catalyst species **Int-C** self-assembling an active chiral pocket whose size and catalytic activity can be tuned by the H-bond interactions and the surrounding functional groups. Therefore, controllable-chiral-pocket-based aryl iodine(III) enables the achievement of numerous highly enantioselective transformations. Naturally, the key to implementing the above goal is the exploration of a concise, efficient, and scalable synthetic route to access the pivotal structure **4**, which can be generated from inexpensive chiral sources. Based on our previous study, chloramphenicol base (ANP, 2-amino-1-(4-nitro-phenyl)propane-1,3-diol), as a privileged and unique chiral scaffold, has been widely applied in asymmetric transformations.[57–60] ANP is the crucial synthon in the industrial production of chloramphenicol (CAP), and only (1*R*,2*R*)-ANP is valuable for the construction of antibacterial active isomer of chloramphenicol, while (1*S*,2*S*)-ANP is left as a chiral waste. Recycling industrial waste is conducive to pharmaceutical synthesis and environmental protection; therefore, (1*S*,2*S*)-ANP is an excellent and perfect chiral source. In view of the low price and availability of amino acids, threonine might also be a suitable scaffold to approach chiral aryl iodine catalysts.[61,62] Guided by all the above-mentioned principles, the key structure **4** could be obtained through an easy-handling and upscaling process, leading to swift construction of the precatalyst library and final access to versatile applications in asymmetric oxidations.

Herein, we have developed a concise, facile, practical, and scalable procedure to access a new library of conformationally flexible aryl iodine catalysts from industrial waste and available chiral amino acid threonine. Significantly, the key intermediate **4** can be obtained in a 100 g scale without column isolation, thereby being smoothly transformed to an aryl iodine library in a large quantity. With our disclosed powerful and recyclable catalysts, various asymmetric oxidative reactions have been achieved, such as oxidative dearomatizations with carbon and oxygen nucleophiles, direct C(sp^2)–H/C(sp^3)–H oxidative cross-coupling reaction, and fluoridation (Fig. 1C). Our findings pave a novel, efficient, and more sustainable way for asymmetric organocatalytic oxidations with hypervalent iodine (III) catalysts towards more and further industrial-scale applications.

Results and discussion

Intrigued by this outlook, we commenced our program on catalyst syntheses. The establishment of the aryl iodine precatalyst library started with the previously known and facilely obtained industrial waste (1*S*,2*S*)-ANP **5**, as summarized in Fig. 2. Thus, amino alcohol **5** was converted to its *tert*-butyl carbamate **6** in 91% yield, and the latter was transformed to the corresponding silyl ether **7** through selective protection at the primary hydroxyl group. Subsequently, a reported Mitsunobu reaction utilizing 2-iodobenzene-1,3-diol **8** and silyl ether **7** enabled an approach to the related diether **Cat-1** accompanied by an intramolecular substituent aziridine **9**. In this step, PPh_3 and DIAD were used in excess, and the separation of **Cat-1** should be facilitated by the column isolation due to the complicated mixture of triphenylphosphine oxide, DIAD, and its reduced byproduct. Therefore, we attempted to perform a concise S_N2 substitution to afford **Cat-1**.[63] Based on our previous work and experimental phenomena, we found that the scaffold of ANP and its derivatives possessed unique solubility (*e.g.*, slightly soluble in methanol), leading to a convenient route without column chromatographic isolation. The revised procedure began with protection to afford a cyclic *N*-Boc sulfamidite, which was subsequently converted to cyclic sulfamidate **10** in 86% yield over three steps from product **6**. An S_N2 substitution of the sodium anion of phenol **8** to the sulfamidate **10** led to a facile nucleophilic cleavage to furnish the intermediate *N*-sulfate, which could be smoothly transformed to **Cat-1** *via* an acid-quenched step. A subsequent *N*-Boc deprotected process was readily achieved, forming a key amine structure **11** (>99.9% ee) up to 106 grams scale. With the high-quality achievement of this upscaling operation, the pivotal scaffold **11** could be successfully transferred to an aryl iodine library bearing abundant precatalysts with different hydrogen bonds, such as amides **Cat-2** to **Cat-4** and **Cat-6** to **Cat-11**, ureas **Cat-14** to **Cat-17**, and sulfamides **Cat-18** to **Cat-21**. Moreover, the catalyst bearing the OTBDPS moiety could readily convert to other kinds of catalysts, such as the ester (**Cat-25** to **Cat-34**) and ether (**Cat-37** to **Cat-40**) substituted precatalysts (for details, see the ESI page of P15†). In particular, the column chromatographic isolation was unnecessary during the whole purification process for synthesizing the ANP scaffold derived precatalyst, which could be obtained *via* recrystallization or precipitation; therefore, our route demonstrated the potential for industrialization. Furthermore, (1*R*,2*R*)-ANP could be smoothly utilized to construct the corresponding precatalyst (**Cat-24**) in high efficiency without column isolation. Notably, D- and L-threonine were also facilely applied to the corresponding aryl iodines (**Cat-5**, **Cat-12** to **Cat-13**, and **Cat-22** to **Cat-23**) through similar procedures, and 5-Me/CO_2Me substituted 2-iodobenzene-1,3-diols smoothly reacted with (1*S*,2*S*)-ANP **5** to furnish the related catalysts **Cat-35** to **Cat-36** (for details, see the ESI page of P16†). The structures of **11**[64] and **Cat-8**[65] were confirmed by single crystal X-ray analysis (for details, see the ESI Fig. 5 and 6†).

With the new versatile class of precatalysts in hand, various asymmetric oxidations were consequently explored to verify the utility of the catalyst library. Firstly, the oxidative spirolactonization (Kita reaction)[40,45,54,66–70] of phenol derivatives, considered a benchmark reaction for examining the catalytic activity of hypervalent iodines, was investigated (Table 1). A series of aryl iodines were loaded to the oxidative conditions, in which *m*-chloroperbenzoic acid (^{m}CPBA) was used as an oxidant at −30 °C (Table 1, entries 1–7). These demonstrated that the 2,4,6-trimethylbenzoyl amide substituted catalyst **Cat-8** was the best catalyst, leading to the spirocyclic chiral product **13a** in 77% yield with 98% ee (Table 1, entry 4). Temperature investigations found elevating the temperature to −20 °C would increase the yield to 82% without erosion of the ee

Published on 24 October 2023. Downloaded on 12/13/2023 3:32:08 AM.

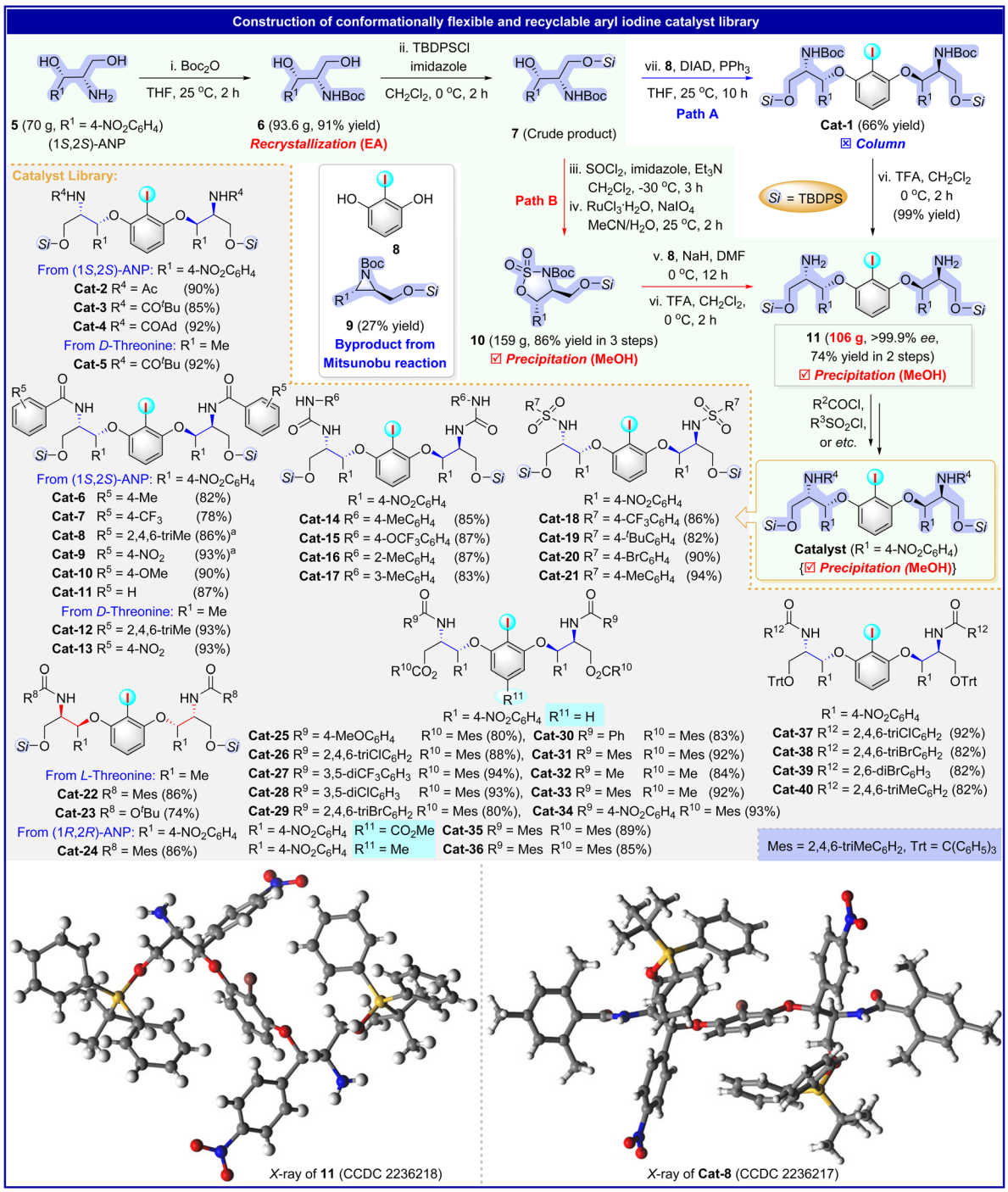

Fig. 2 The general procedure for aryl iodine precatalyst synthesis. [a] Reagents and conditions: (i) Boc_2O (1.05 equiv.), THF, 25 °C, 2 h, 91%; (ii) TBDPSCl (1.05 equiv.), imidazole (1.3 equiv.), CH_2Cl_2, 0 °C, 2 h; (iii) $SOCl_2$ (1.2 equiv.), imidazole (3 equiv.), Et_3N (2.4 equiv.), −30 °C, 3 h; (iv) $NaIO_4$ (1.1 equiv.), $RuCl_3{\cdot}H_2O$ (1 mol%), $MeCN/H_2O$ (1 : 1), 25 °C, 2 h, 86% (three steps); (v) **8** (0.5 equiv.), NaH (1.2 equiv.), DMF, 0 °C, 12 h; (vi) TFA/DCM (1 : 4), 2 h, 74% (two steps); (vii) DIAD (2.3 equiv.), PPh_3 (2.7 equiv.), THF, 25 °C, 10 h, 66%.

value (Table 1, entries 4, 8 and 9). When the TBDPS substituent on the side arm of the catalyst was changed to the acetyl (**Cat-33**) with less steric hindrance, the efficiency of accessing desired product **13a** would be decreased (Table 1, entries 9 and 10). Solvent investigations demonstrated that CH_2Cl_2 was the best solvent in this oxidative transformation (Table 1, entries 8, 11 and 12). When five equivalent amounts of ethanol were added as an additive to stabilize the hypervalent iodine(III) intermediate,[54] product **13a** would be furnished in 92% yield with 98% ee (Table 1, entry 13). When a smaller amount of precatalyst was loaded, the lower yield of compound **13a** was afforded (Table 1, entries 13–15). Increasing the

 This journal is © The Royal Society of Chemistry 2023

Published on 24 October 2023. Downloaded on 12/13/2023 3:32:08 AM.

Table 1 Optimization of the enantioselective oxidative dearomatization[a]

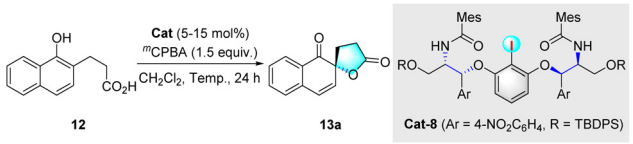

Entry	Cat (mol%)	Solvent	Temp. (°C)	Yield[b] (%)	ee[c] (%)
1	**Cat-1** (15)	CH_2Cl_2	−30	45	85
2	**Cat-2** (15)	CH_2Cl_2	−30	66	79
3	**Cat-6** (15)	CH_2Cl_2	−30	56	86
4	**Cat-8** (15)	CH_2Cl_2	−30	77	98
5	**Cat-9** (15)	CH_2Cl_2	−30	52	90
6	**Cat-11** (15)	CH_2Cl_2	−30	47	86
7	**Cat-21** (15)	CH_2Cl_2	−30	35	75
8	**Cat-8** (15)	CH_2Cl_2	−20	82	98
9	**Cat-8** (15)	CH_2Cl_2	0	87	96
10	**Cat-33** (15)	CH_2Cl_2	0	80	92
11	**Cat-8** (15)	Toluene	−20	77	96
12	**Cat-8** (15)	EtOAc	−20	44	87
13	**Cat-8 (15)**	**CH_2Cl_2 + EtOH[d]**	**−20**	**92**	**98**
14	**Cat-8** (10)[e]	CH_2Cl_2 + EtOH[d]	−20	80	98
15	**Cat-8** (5)[f]	CH_2Cl_2 + EtOH[d]	−20	72	98
16	**Cat-8** (15)	CH_2Cl_2 + EtOH[g]	−20	92	96

[a] **12** (0.2 mmol, 1.0 equiv.), **Cat** (0.03 mmol, 15 mol%), and ^{m}CPBA (0.3 mmol, 1.5 equiv.) were stirred in CH_2Cl_2 (10 mL) at −30 to 0 °C for 24 h. [b] Isolated yield. [c] The ee value was determined by chiral HPLC. [d] EtOH (1 mmol, 5 equiv.) was added. [e] **Cat-8** (0.02 mmol, 10 mol%) was added. [f] **Cat-8** (0.01 mmol, 5 mol%) was added. [g] CH_2Cl_2 (5 mL) and EtOH (1 mmol, 5 equiv.) were added.

solvent concentration led to a slight reduction of the enantioselectivity (Table 1, entry 16).

With the optimized conditions in hand, we examined the scope of the Kita reaction (Scheme 1). We initiated our efforts with substituted 3-(1-hydroxynaphthalen-2-yl)propanoic acids **12** to this transformation. 4-Halogeno substituted substrates were smoothly converted to the desired products in high yields with excellent enantioselectivities (Scheme 1, **13b–13c**). The feedstocks bearing electron-withdrawing groups (EWGs), such as benzoyl and acetyl, were successfully transformed to the products **13d–13e** in good chemical yields with high enantioselectivities. The 1-naphthol derivatives substituted with both 4-phenyl and 4-benzyl were tolerant of the standard conditions, leading to the desired products with 96% ee and good chemical yields (Scheme 1, **13f–13g**). The utilization of other substrates bearing 4-alkyl and 6-methoxyl gave the corresponding products **13h–13l** in moderate to high yields with excellent enantioselectivities. Subsequently, 3-(2-hydroxynaphthalen-1-yl)propanoic acids containing different kinds of functional groups were well tolerated to generate the counterparts **13m–13o** in good yields with excellent ee values. Gratefully, the gram-scale operation was successfully achieved by using lower catalyst loading of **Cat-8** (5 mol%), leading to **13a** in 1.19 g with 80% yield and 99% ee *via* recrystallization along with recovery of the precatalyst in 96% yield (for details, please see the ESI page of P50†). Moreover, the corresponding catalyst **Cat-24** and **Cat-22** prepared from (1*R*,2*R*)-ANP and L-threonine could facilely be utilized in this reaction system, leading to the generation of products **13g** and **13i** with opposite configurations in high efficiency, respectively. Importantly, our designed conformationally flexible chiral organoiodine(III) catalyst could also be applied to the oxidative cyclization of alcohols. Because substrate-incorporated EWGs presented higher reactivity in Ciufolini's work,[70] we focused on investigating the lower reactive compounds bearing electron-donating groups (EDGs). All these substrates with EDGs could produce the desired products **14b–14f** and **14j** in moderate to high yields with excellent enantioselectivities. Compared with the reported catalysts, our catalyst presented the highest efficiency in this transformation (**14g–14i**), illustrating the proposed transition state would be more stable to inhibit its dissociation, which might result from its peculiar chiral pocket and intramolecular H-bond interactions.

Encouraged by the high efficiency of our developed catalyst in the oxidative dearomatization of substituted naphthols, we continued to expand the applications of our catalyst library to other types of transformations (Scheme 2). Firstly, the *C*-attacked asymmetric spirocyclization of 1-hydroxy-*N*-aryl-2-naphthamide derivatives **15** was further employed to access functionalized spirooxindoles **16** bearing an all-carbon stereogenic center (Scheme 2-(1)). In this reaction, the selected precatalyst **Cat-9** displayed outstanding reactivity to furnish the desired products **16a–16d** in moderate to good yields with excellent enantioselectivities under milder conditions (−10 °C) using ^{m}CPBA as oxidant, trifluoroethanol (TFE) and water as additives, and nitromethane as solvent (for details, please see the ESI Table 2†). Therefore, our catalyst possessed higher stereoselective efficiency than the previous catalyst reported by Gong and co-workers,[71] which further demonstrated the H-bond donor and the multiple tunable sites installed on the chiral pocket were necessary. To facilitate the diversified application of our catalyst library, the direct C(sp^2)–H/C(sp^3)–H cross-coupling was subsequently engaged (Scheme 2-(2)), in which the anilide derivatives **17** was smoothly transformed to the spirooxindoles **18** by utilizing pivalamido-substituted precatalyst **Cat-3**, ^{m}CPBA as oxidant, CF_3CO_2H and H_2O as additives, and acetonitrile as solvent at room temperature (for details, please see the ESI Table 3†). In this scenario, the more secure and available oxidant ^{m}CPBA was employed to replace CH_3CO_3H, which was loaded in the previous work.[22] The confused spirooxindoles **18a–18f** could be furnished in moderate to high yields (41–80%) with high enantioselectivities (82–90% ee). Hence, our developed iodine catalyst further possessed high reactivity and practicability.

The installation of fluorine atoms on organic molecules is a significant approach towards the adjustment of molecular properties, such as lipophilicity, membrane permeability, biokinetics, and biodynamics, within agrochemicals, pharmaceuticals, and materials.[72–77] Furthermore, hypervalent iodine catalysis has been successfully utilized in asymmetric fluorination, which provides a concise and inexpensive approach to access potential pharmaceuticals. Therefore, the development of a

Published on 24 October 2023. Downloaded on 12/13/2023 3:32:08 AM.

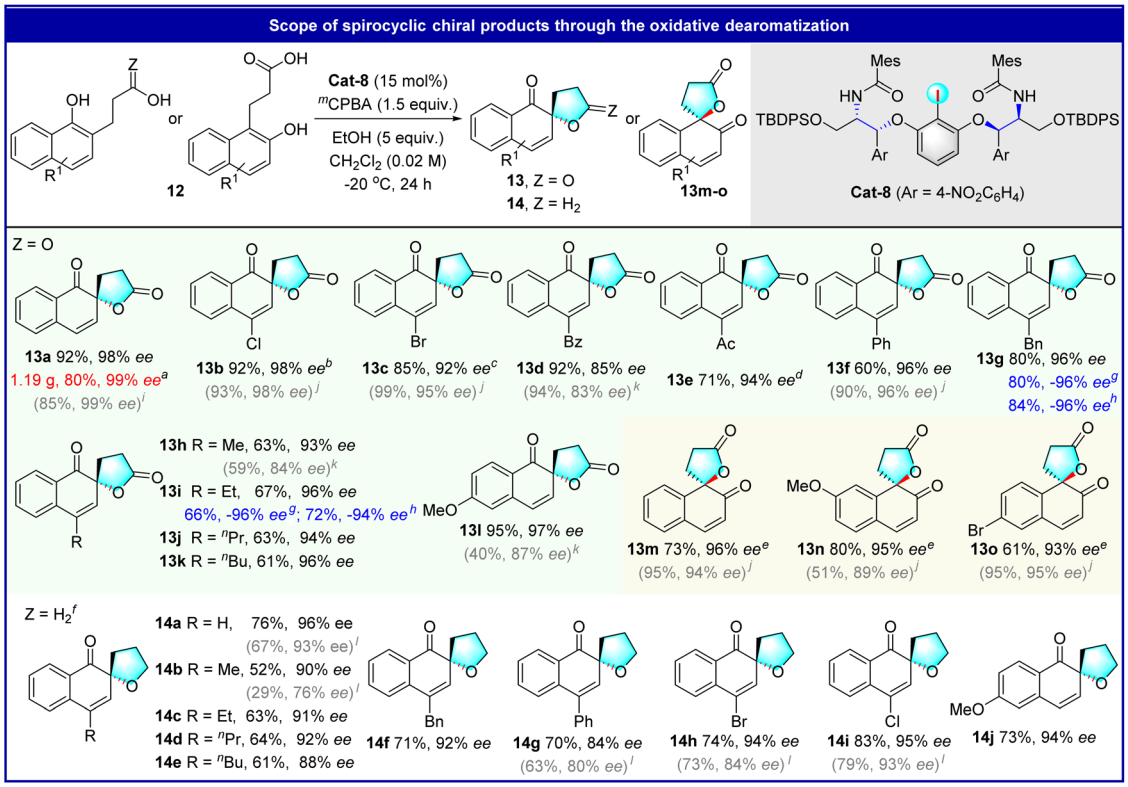

Scheme 1 Applications of the new aryl iodine catalyst in oxidative dearomatization. **12** (0.2 mmol, 1.0 equiv.), **Cat-8** (0.03 mmol, 15 mol%), ^{m}CPBA (0.3 mmol, 1.5 equiv.), and EtOH (1 mmol, 5 equiv.) were stirred in CH_2Cl_2 (10 mL) at −20 °C for 24 h. Isolated yield. The ee value was determined by chiral HPLC. [a] **12** (7 mmol, 1.0 equiv.), **Cat-8** (0.35 mmol, 5 mol%), ^{m}CPBA (8.3 mmol, 1.2 equiv.), and EtOH (35 mmol, 5 equiv.) were stirred in CH_2Cl_2 (100 mL) at −20 °C for 48 h; the ee value and yield were determined after recrystallization. [b] Without EtOH. [c] Stirred at 0 °C. [d] Stirred at 0 °C for 80 h. [e] **12** (0.2 mmol, 1.0 equiv.), **Cat-8** (0.03 mmol, 15 mol%), ^{m}CPBA (0.3 mmol, 1.5 equiv.), and HFIP (10 mmol, 50 equiv.) were stirred in CH_2Cl_2 (10 mL) at −20 °C for 24 h. [f] Stirred for 16 h. [g] **Cat-24** was used. [h] **Cat-22** was used. [i] Reported in ref. 49. [j] Reported in ref. 54. [k] Reported in ref. 40. [l] Reported in ref. 70.

new catalyst to achieve the formation of chiral fluorinated molecules is unquestionably beneficial. Our catalyst library was subsequently loaded to the enantioselective fluorination of keto esters **19** (Scheme 3).[46,78] To our delight, the aryl iodine **Cat-38** bearing large steric hindrance groups was the optimized catalyst to access asymmetric fluorination with high efficiency, in which 2,4,6-tribromobenzoyl and triphenylmethyl (Trt) were substituted on the amine and ether moieties, respectively (for details, please see the ESI Table 4†). Hence, the excellent ee values and moderate yields of desired products **20a–20k** could be obtained.

Inspired by the concise and utility procedure of catalyst construction, the recovery and recycling of our developed catalyst might be feasible. A significant step in evaluating the sustainability characteristics of the precatalyst **Cat-8** was the assessment of its recyclability (Scheme 4). To this end, a sample of **Cat-8** was repeatedly utilized in the reaction of substrate **12a** in the presence of ^{m}CPBA, ethanol, and CH_2Cl_2. At the end of each reaction cycle, the reaction mixture was quenched in the sequence of saturated $Na_2S_2O_3$ and $NaHCO_3$ aqueous solution. The organic layer was then extracted with CH_2Cl_2, washed with brine and dried over anhydrous Na_2SO_4. The mixture was concentrated *in vacuo*; the residue was subsequently dissolved by 30 mL of MeOH, and H_2O (10 mL) was finally added to precipitate the catalyst, which could enter the next cycle. The filtrate was concentrated *in vacuo* to get the crude product that could be further recrystallized by the mixture (10 mL, 1 : 300 volume ratio) of ethyl acetate and petroleum ether (for details, please see the ESI page of P48†). Delightfully, **Cat-8** presented considerably high reactivity and selectivity in 10 consecutive cycles, therefore indicating high robustness. Notably, aryl iodine **Cat-8** was easily and efficiently recovered from the reaction mixture with high efficiency (all cycles >96% yield) over the whole operation period, while enantiospecificity of product **13a** steadily maintained in 97% ee. Around 5.37 g (combined weight) of pure **13a** was isolated over ten-cycle operations, which represented an accumulated TON of 83.6. These implements demonstrated our designed catalysts possessed high potential for industrial applications.

Based on our designed strategy to construct a chiral aryl iodine catalyst, both the H-bond interaction and the tunable chiral pocket are essential (Fig. 1B, **Int-C**). To validate our hypothesis, controlled experiments were conducted in turn (Scheme 5). Firstly, when the N–H bonds of the amide moiety

 This journal is © The Royal Society of Chemistry 2023

Published on 24 October 2023. Downloaded on 12/13/2023 3:32:08 AM.

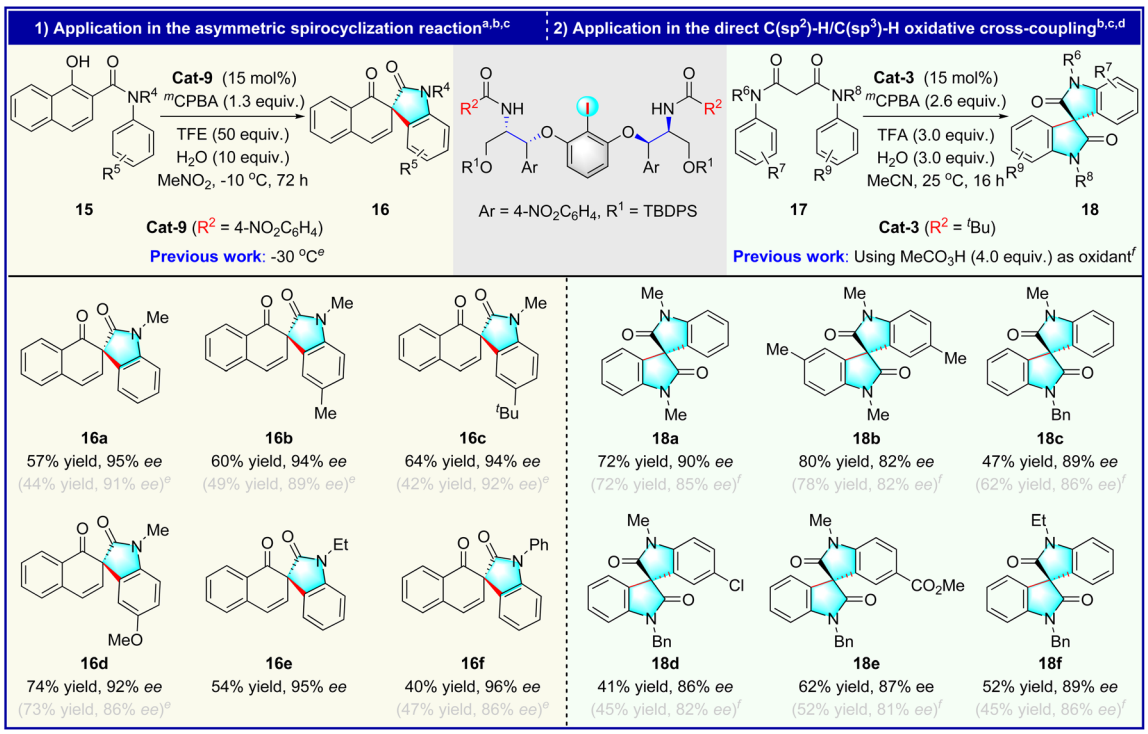

Scheme 2 Applications of the aryl iodine catalyst library in the oxidative spirolactonization and direct C(sp^2)–H/C(sp^3)–H cross-coupling. [a] **15** (0.2 mmol, 1.0 equiv.), **Cat-9** (0.03 mmol, 15 mol%), ^{m}CPBA (0.26 mmol, 1.3 equiv.), TFE (10 mmol, 50 equiv.), and H_2O (2 mmol, 10 equiv.) were stirred in $MeNO_2$ (3 mL) at −10 °C for 72 h. [b] Isolated yield. [c] The ee value was determined by chiral HPLC. [d] **17** (0.2 mmol, 1.0 equiv.), **Cat-3** (0.03 mmol, 15 mol%), ^{m}CPBA (0.52 mmol, 2.6 equiv.), TFA (0.6 mmol, 3 equiv.), and H_2O (0.6 mmol, 3 equiv.) were stirred in MeCN (3 mL) at 25 °C for 16 h. [e] Reported in ref. 71. [f] Reported in ref. 22.

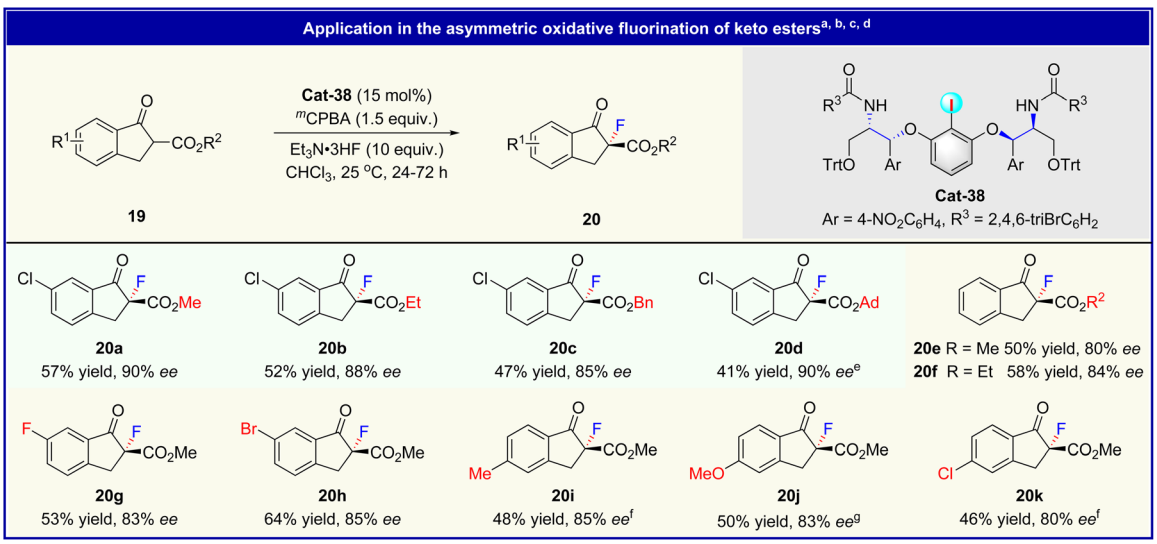

Scheme 3 Application of the aryl iodine catalyst library in the oxidative fluorination of keto esters. [a] **19** (0.2 mmol, 1.0 equiv.), **Cat-38** (0.03 mmol, 15 mol%), ^{m}CPBA (0.3 mmol, 1.5 equiv.), and $Et_3N{\cdot}3HF$ (3 mmol, 10 equiv.) were stirred in $CHCl_3$ (8 mL) at 25 °C for 24 h. [b] Isolated yield. [c] The ee value was determined by chiral HPLC. [d] Absolute configurations were reported in ref. 78. [e] Ad = 1-adamantanoxy. [f] 48 h. [g] 72 h.

on the optimized catalysts (**Cat-41**, **Cat-43**, **Cat-45**, and **Cat-47**) were changed to N–Me bonds, the yield and enantioselectivity of the corresponding products (**13a**, **16a**, **18a**, and **20a**) would sharply decline, indicating the H-bond interactions in the key species were fundamental. D-Threoninol derived aryl iodine catalysts (**Cat-12**, **Cat-13**, **Cat-5**, and **Cat-48**) were then applied to replace the (1*S*,2*S*)-ANP substituted analogues, leading to a slight or dramatic decrease in the reactivities and enantio-

Published on 24 October 2023. Downloaded on 12/13/2023 3:32:08 AM.

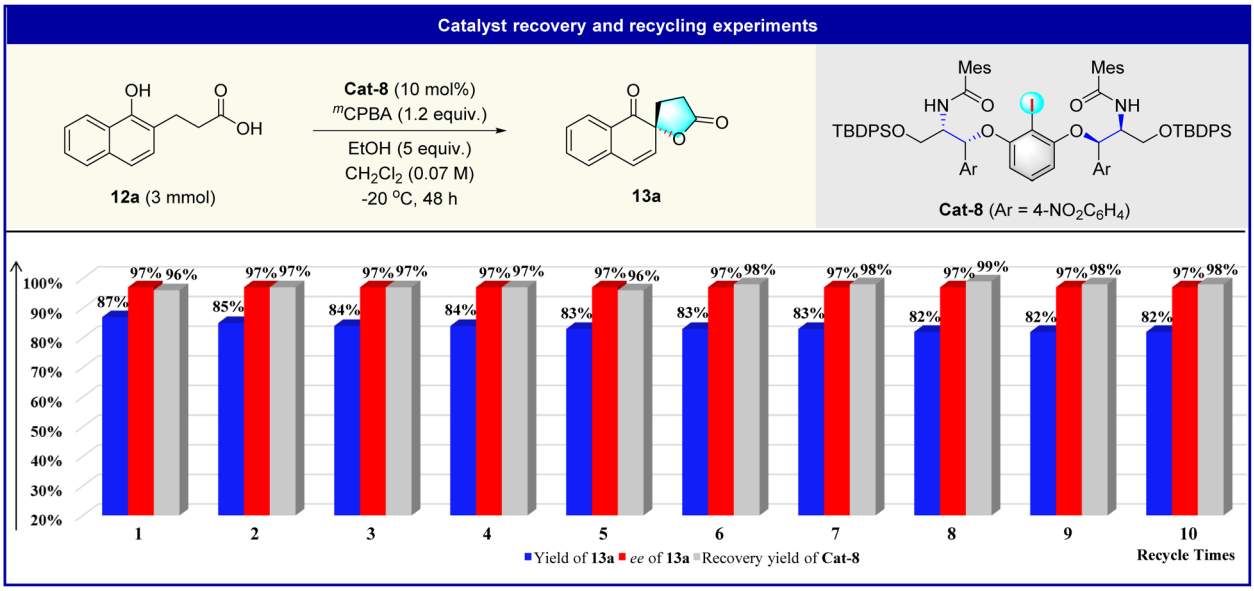

Scheme 4 Catalyst recovery from and recycling experiments for oxidative dearomatization. **12a** (3 mmol, 1.0 equiv.), **Cat-8** (0.3 mmol, 10 mol%), ^{m}CPBA (3.6 mmol, 1.2 equiv.), and EtOH (15 mmol, 5 equiv.) were stirred in CH_2Cl_2 (43 mL) at −20 °C for 24 h. Isolated yield. The ee value was determined by chiral HPLC. Catalyst was precipitated by the mixture of MeOH (30 mL) and H_2O (10 mL). Product was recrystallized by the mixture (10 mL, 1 : 300 volume ratio) of ethyl acetate and petroleum ether.

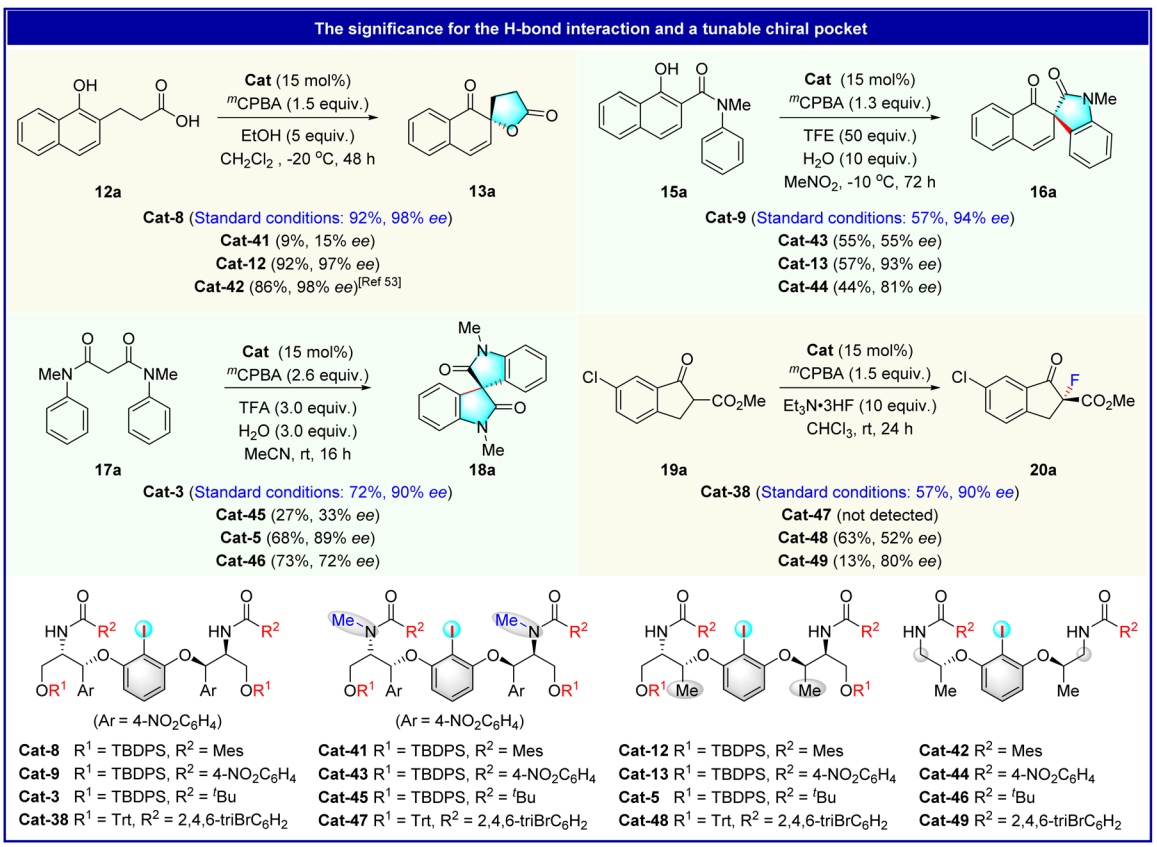

Scheme 5 The significance of the H-bond interaction and tunable chiral pocket.

This journal is © The Royal Society of Chemistry 2023

Published on 24 October 2023. Downloaded on 12/13/2023 3:32:08 AM.

selectivities. These demonstrated that multi-chiral centers were significant for the new catalyst scaffold. Finally, when the substituent R^2 ($CH_2OTBDPS$ or CH_2OTrt) on the side arm of related catalysts (**Cat-8**, **Cat-9**, **Cat-3**, and **Cat-38**) were replaced by H atom (**Cat-42**, **Cat-44**, **Cat-46**, and **Cat-49**), the ee values of desired products would be reduced dramatically in most cases, which indicated that the chiral pocket formed from the structure of multi chiral centers *via* self-assembly was essential. Hence, both the H-bond interactions and tunable chiral pocket were indispensable for these types of catalyst skeletons.

Conclusions

In conclusion, we have developed a versatile and efficient synthetic process that allows the construction of various new conformationally flexible and recyclable aryl iodine catalysts bearing H-bond donors and a tunable chiral pocket. The synthesis of the key intermediate for the formation of the catalyst library can be upscaled to more than 100 grams and is column-isolation-free. Furthermore, our designed catalysts have achieved a series of highly enantioselective oxidative transformations, for example, *C*-/*O*-attacked intramolecular asymmetric dearomatization, direct $C(sp^2)$–$H/C(sp^3)$–H oxidative cross-coupling and fluoridation, to synthesize valuable functionalized products from different types of feedstocks. The catalyst recycling experiments and gram-scale operations of catalyst preparation are smoothly carried out to validate the great practicability of our protocol. Control experiments demonstrate that H-bond donors and the tunable chiral pocket are essential components for the aryl iodine catalysts. The promising utilities of these classes of chiral aryl iodine scaffolds in catalytic asymmetric oxidations and pharmaceutical syntheses are currently under investigation in our laboratories and will be reported in due course.

Author contributions

X. X. and F.-E. C. designed the project. X. X. and H.-J. Z. designed and carried out the experiments. Y.-P. Y., B. C., X. W., H. Z., and J.-A. C. contributed to part experiments. T. Z. and J. Z. carried out the DFT studies. X. X. and F.-E. C. discussed the results, contributed to writing the manuscript, and commented on the manuscript. All authors approved the final version of the manuscript for submission.

Conflicts of interest

There are no conflicts to declare.

Acknowledgements

This work was supported by the National Natural Science Foundation of China (no. 22208302) and the Natural Science Foundation of Zhejiang Province of China (no. LQ21B020006, ZJ2022039). We thank Dr Wai-Lun Chan for helpful discussions, as well as proofreading of the manuscript and ESI.†

Notes and references

1 P. J. Stang and V. V. Zhdankin, *Chem. Rev.*, 1996, **96**, 1123–1178.
2 V. V. Zhdankin and P. J. Stang, *Chem. Rev.*, 2002, **102**, 2523–2584.
3 T. Wirth, *Angew. Chem., Int. Ed.*, 2005, **44**, 3656–3665.
4 V. V. Zhdankin and P. J. Stang, *Chem. Rev.*, 2008, **108**, 5299–5358.
5 E. A. Merritt and B. Olofsson, *Angew. Chem., Int. Ed.*, 2009, **48**, 9052–9070.
6 M. Uyanik and K. Ishihara, *Chem. Commun.*, 2009, **45**, 2086–2099.
7 T. Dohi and Y. Kita, *Chem. Commun.*, 2009, **45**, 2073–2805.
8 L. F. Silva and B. Olofsson, *Nat. Prod. Rep.*, 2011, **28**, 1722–1754.
9 A. Yoshimura and V. V. Zhdankin, *Chem. Rev.*, 2016, **116**, 3328–3435.
10 S. Maiti, M. T. Alam, A. Bal and P. Mal, *Adv. Synth. Catal.*, 2019, **361**, 4401–4425.
11 A. Bauer and N. Maulide, *Chem. Sci.*, 2021, **12**, 853–864.
12 S. Wang, R. Li, S. Chen, G. Mao, W. Shao and G. Deng, *Green Synth. Catal.*, 2023, **4**, DOI: **10.1016/j.gresc.2023.01.002**.
13 A. Parra and S. Reboredo, *Chem. – Eur. J.*, 2013, **19**, 17244–17260.
14 F. Berthiol, *Synthesis*, 2015, 587–603.
15 A. Claraz and G. Masson, *Org. Biomol. Chem.*, 2018, **16**, 5386–5402.
16 A. Flores, E. Cots, J. Bergès and K. Muñiz, *Adv. Synth. Catal.*, 2019, **361**, 2–25.
17 A. Parra, *Chem. Rev.*, 2019, **119**, 12033–12088.
18 M. Uyanik and K. Ishihara, *TCI Mail*, 2019, **182**, 2–14.
19 Y. Wang, B. Yang, X. Wu and Z. Wu, *Synthesis*, 2021, 889–903.
20 S. Meyer, J. Häfliger and R. Gilmour, *Chem. Sci.*, 2021, **12**, 10686–10695.
21 F. V. Singh, S. E. Shetgaonkar, M. Krishnan and T. Wirth, *Chem. Soc. Rev.*, 2022, **51**, 8102–8139.
22 H. Wu, Y. He, L. Xu, D. Zhang and L. Gong, *Angew. Chem., Int. Ed.*, 2014, **53**, 3466–3469.
23 S. Haubenreisser, T. H. Wöste, C. Martínez, K. Ishihara and K. Muñiz, *Angew. Chem., Int. Ed.*, 2016, **55**, 413–417.
24 E. M. Woerly, S. M. Banik and E. N. Jacobsen, *J. Am. Chem. Soc.*, 2016, **138**, 13858–13861.
25 K. Muñiz, L. Barreiro, R. M. Romero and C. Martínez, *J. Am. Chem. Soc.*, 2017, **139**, 4354–4357.
26 K. M. Mennie, S. M. Banik, E. C. Reichert and E. N. Jacobsen, *J. Am. Chem. Soc.*, 2018, **140**, 4797–4802.

Published on 24 October 2023. Downloaded on 12/13/2023 3:32:08 AM.

27 Q. Wang, M. Lübcke, M. Biosca, M. Hedberg, M. Eriksson, F. Himo and K. J. Szabó, *J. Am. Chem. Soc.*, 2020, **142**, 20048–20057.
28 J. C. Sarie, C. Thiehoff, J. Neufeld, C. G. Daniliuc and R. Gilmour, *Angew. Chem., Int. Ed.*, 2020, **59**, 15069–15075.
29 S. Meyer, J. Häfliger, M. Schäfer, J. J. Molloy, C. G. Daniliuc and R. Gilmour, *Angew. Chem., Int. Ed.*, 2021, **60**, 6430–6434.
30 C. Wata and T. Hashimoto, *J. Am. Chem. Soc.*, 2021, **143**, 1745–1751.
31 M. Schäfer, T. Stünkel, C. G. Daniliuc and R. Gilmour, *Angew. Chem., Int. Ed.*, 2022, **61**, e202205508.
32 J. Häfliger, O. O. Sokolova, M. Lenz, C. G. Daniliuc and R. Gilmour, *Angew. Chem., Int. Ed.*, 2022, **61**, e202205277.
33 S. M. Banik, J. W. Medley and E. N. Jacobsen, *Science*, 2016, **353**, 51–54.
34 B. Zhou, M. K. Haj, E. N. Jacobsen, K. N. Houk and X. Xue, *J. Am. Chem. Soc.*, 2018, **140**, 15206–15218.
35 D. Zhang, Y. Zhang, H. Wu and L. Gong, *Angew. Chem., Int. Ed.*, 2019, **58**, 7450–7453.
36 H. A. Sharma, K. M. Mennie, E. E. Kwan and E. N. Jacobsen, *J. Am. Chem. Soc.*, 2020, **142**, 16090–16096.
37 M. D. Levin, J. M. Ovian, J. A. Read, M. S. Sigman and E. N. Jacobsen, *J. Am. Chem. Soc.*, 2020, **142**, 14831–14837.
38 W. Zhu, X. Zhen, J. Wu, Y. Cheng, J. An, X. Ma, J. Liu, Y. Qin, H. Zhu, J. Xue and X. Jiang, *Nat. Commun.*, 2021, **12**, 3957.
39 R. D. Richardson, T. K. Page, S. Altermann, S. M. Paradine, A. N. French and T. Wirth, *Synlett*, 2007, 538–542.
40 M. Uyanik, T. Yasui and K. Ishihara, *Angew. Chem., Int. Ed.*, 2010, **49**, 2175–2177.
41 H. Zheng, L. Cai, L. Pan, M. Uyanik, K. Ishihara and X. Xue, *J. Am. Chem. Soc.*, 2023, **145**, 7301–7312.
42 J. Yu, J. Cui, X. Hou, S. Liu, W. Gao, S. Jiang, J. Tian and C. Zhang, *Tetrahedron: Asymmetry*, 2011, **22**, 2039–2055.
43 P. Mizar, A. Laverny, M. El-Sherbini, U. Farid, M. Brown, F. Malmedy and T. Wirth, *Chem. – Eur. J.*, 2014, **20**, 9910–9913.
44 M. Bekkaye and G. Masson, *Synthesis*, 2016, 302–312.
45 T. Dohi, T. Sasa, K. Miyazaki, M. Fujitake, N. Takenaga and Y. Kita, *J. Org. Chem.*, 2017, **82**, 11954–11960.
46 Y. Wang, H. Yuan, H. Lu and W. Zheng, *Org. Lett.*, 2018, **20**, 2555–2558.
47 T. Hashimoto, Y. Shimazaki, Y. Omatsu and K. Maruoka, *Angew. Chem., Int. Ed.*, 2018, **57**, 7200–7204.
48 K. Antien, L. Pouységu, D. Deffieux, S. Massip, P. A. Peixoto and S. Quideau, *Chem. – Eur. J.*, 2019, **25**, 2852–2855.
49 A. H. Abazid and B. J. Nachtsheim, *Angew. Chem., Int. Ed.*, 2020, **59**, 1479–1484.
50 A. Sreenithya, C. Patel, C. M. Hadad and C. M. Sunoj, *ACS Catal.*, 2017, **7**, 4189–4196.
51 M. Uyanik, T. Yasui and K. Ishihara, *Angew. Chem., Int. Ed.*, 2013, **52**, 9215–9218.
52 E. Cots, J. Rintjema, F. Bravo and K. Muñiz, *Org. Lett.*, 2021, **23**, 6429–6434.
53 M. Uyanik, N. Sasakura, M. Mizuno and K. Ishihara, *ACS Catal.*, 2017, **7**, 872–876.
54 M. Uyanik, T. Yasui and K. Ishihara, *J. Org. Chem.*, 2017, **82**, 11946–11953.
55 T. Suzuki, S. Watanabe, M. Uyanik, K. Ishihara, S. Kobayashi and K. Tanino, *Org. Lett.*, 2018, **20**, 3919–3922.
56 M. Uyanik, S. Ishizaki and K. Ishihara, *Org. Synth.*, 2021, **98**, 1–27.
57 S. X. Wang and F. E. Chen, *Adv. Synth. Catal.*, 2009, **351**, 547–552.
58 H. Wang, L. Yan, Y. Wu, Y. Lu and F. Chen, *Org. Lett.*, 2015, **17**, 5452–5455.
59 L. Yan, H. Wang, W. Chen, Y. Tao, K. J. Jin and F. E. Chen, *ChemCatChem*, 2016, **8**, 2249–2253.
60 Y. Xiao and F. E. Chen, *ChemCatChem*, 2019, **11**, 2043–2053.
61 T. Wang, X. Han, F. Zhong, W. Yao and Y. Lu, *Acc. Chem. Res.*, 2016, **49**, 1369–1378.
62 H. Ni, W. Chan and Y. Lu, *Chem. Rev.*, 2018, **118**, 9344–9411.
63 J. F. Bower, P. Szeto and T. Gallagher, *Org. Lett.*, 2007, **9**, 3283–3286.
64 CCDC 2236218 (**11**):† $C_{56}H_{61}IN_4O_8Si_2$, MW=1101.16, orthorhombic, space group $P2_12_12$, final R indexes [$I \geq 2\sigma(I)$], R_1=0.0439, wR_2=0.1027, R indexes (all data), R_1=0.0724, wR_2=0.1185, a=28.216(9) Å, b=13.252(2) Å, c=14.528(3) Å, α=90°, β=90°, γ=90°, V=5432(2) Å^3, Z=4, reflections collected: 94 001, independent reflections: 15 884 [R_{int}=0.0513, R_{sigma}=0.0406].
65 CCDC 2236217 (**Cat-8**):† $C_{76}H_{81}IN_4O_{10}Si_2$, MW=1393.52, orthorhombic, space group $P2_12_12$, final R indices [$I \geq 2\sigma(I)$], R_1=0.0245, wR_2=0.0560, R indices (all data), R_1=0.0285, wR_2=0.0584, a=13.3936(3) Å, b=27.4740(6) Å, c=9.5840(2) Å, α=90°, β=90°, γ=90°, V=3526.68(13) Å^3, Z=2, reflections collected: 54 725, independent reflections: 8123 [R_{int}=0.0361, R_{sigma}=0.0251].
66 T. Dohi, A. Maruyama, N. Takenaga, K. Senami, Y. Minamitsuji, H. Fujioka, S. B. Caemmerer and Y. Kita, *Angew. Chem., Int. Ed.*, 2008, **47**, 3787–3790.
67 T. Dohi, N. Takenaga, T. Nakae, Y. Toyoda, M. Yamasaki, M. Shiro, H. Fujioka, A. Maruyama and Y. Kita, *J. Am. Chem. Soc.*, 2013, **135**, 4558–4566.
68 C. Maichle-Mössmer, M. A. Pericàs and B. J. Nachtsheim, *Adv. Synth. Catal.*, 2017, **359**, 2931–2941.
69 M. Ogasawara, H. Sasa, H. Hu, Y. Amano, H. Nakajima, N. Takenaga, N. Nakajima, Y. Kita, T. Takahashi and T. Dohi, *Org. Lett.*, 2017, **19**, 4102–4105.
70 N. Jain, S. Xu and M. A. Ciufolini, *Chem. – Eur. J.*, 2017, **23**, 4542–4546.
71 D. Zhang, L. Xu, H. Wu and L. Gong, *Chem. – Eur. J.*, 2015, **21**, 10314–10317.
72 K. Müller, C. Faeh and F. Diederich, *Science*, 2007, **317**, 1881–1886.
73 S. Purser, P. R. Moore, S. Swallow and V. Gouverneur, *Chem. Soc. Rev.*, 2008, **37**, 320–330.
74 W. K. Hagmann, *J. Med. Chem.*, 2008, **51**, 4359–4369.

 This journal is © The Royal Society of Chemistry 2023

75 B. Manteau, S. Pazenok, J. Vors and F. R. J. Leroux, *Fluorine Chem.*, 2010, **131**, 140–158.
76 T. Furuya, A. S. Kamlet and T. Ritter, *Nature*, 2011, **473**, 470–477.
77 X. Zhang, Y. Cheng, X. Zhao, Z. Cao, X. Xiao and Y. Xu, *Org. Chem. Front.*, 2021, **8**, 2315–2327.
78 R. Pluta, P. E. Krach, L. Cavallo, L. Falivene and M. Rueping, *ACS Catal.*, 2018, **8**, 2582–2588.

Published on 24 October 2023. Downloaded on 12/13/2023 3:32:08 AM.